On the Classification of the Electric Field Spectroscopies: Application to Raman Scattering

Jason C. Kirkwood, Darin J. Ulness,† and A.C. Albrecht*

Department of Chemistry, Baker Laboratory, Cornell University, Ithaca, New York 14853

Received: July 22, 1999; In Final Form: September 20, 1999

Modern electric field-based spectroscopies, both linear and nonlinear, are assigned to two classes having strongly differentiating properties. In one, Class I, the language of photons absorbed and emitted appears naturally. In Class II, the basic physics is sorted out at the field level itself and the language of wave-mixing is used. So, among other things, the phase of the material response function becomes an issue for Class II spectroscopies. Field "generators" together with density matrix evolution diagrams are found to be useful tools for isolating any given spectroscopy from the great many that may appear at any given order in the light−matter interaction. By way of example, it is shown how the generators and diagrams allow one to extract all of the Raman scattering processes as a distinct subgroup of a much larger set of spectroscopies that occur at various orders. Each is assigned either to Class I or II and identified with key evolution diagrams.

I. Introduction

The many modern electric field-based spectroscopies are routinely classified as being "linear" or "nonlinear". This follows from the perturbative approach to light−matter interactions involving resonances. The leading term of such interaction involves the electric field component of the electromagnetic (EM) radiation—extending from the microwave into the vacuum ultraviolet. And, except for very high intensities, matrix elements of the inner product of the incident electric field vector and the material dipole vector operator have magnitudes (the Rabi energy) that are sufficiently weak (compared to the Bohr energies of the system) to validate a perturbative approach in orders of the Rabi energy of the light (or, equivalently, in orders of the incident electric field). Accordingly, this perturbative ordering alone has invited the general classification of spectroscopies into linear and nonlinear.

However, a less frequently used categorization, but nevertheless an apparently quite useful one is to define any given spectroscopy (linear or nonlinear) as being *active* or *passive*.[1,2] The *active* spectroscopies are those in which the principal event is a change of state population in the material. In order to conserve energy, this must be accompanied by an appropriate change of photon numbers in the light field. Thus, net energy is transferred between light and matter in a manner that survives averaging over many cycles of the perturbing light waves. We call these the Class I spectroscopies. For these, the language of photons absorbed and emitted is invariably used. They constitute all of the well-known absorption and emission spectroscopies—whether they be one-photon or multiphoton.

The *passive* spectroscopies, here called Class II, come from the momentary exchange of energy between light and matter that induces a macroscopically coherent, oscillating, electrical polarization (an oscillating electric dipole density wave) in the material. As long as this coherence is sustained, such polarization can serve as a source term in the wave equation for the electric field. A new (EM) field (the signal field) is produced at the frequency of the oscillating polarization in the sample. The frequency or "color" of this new field is usually (but not always) different from the spectral content of the incident field. Provided the polarization wave retains some coherence, and matches the signal field in direction and wavelength (the "phase matching" condition), the new EM field can build up and escape the sample and ultimately be measured "in quadrature" (as photons). This new field may be detected as its own mod-square (or self-quadrature) called "homodyne" detection, or it may be converted to photons through its superposition with a laboratory field, a "local oscillator" field, called "heterodyne" detection. In their extreme form, when no material resonances are operative, the Class II events (without resonances "spectroscopies" is a misnomer) will alter only the states of the EM radiation and none of the material. In this case, the material acts *passively* while "catalyzing" alterations in the radiation. When resonances are present, Class II events become spectroscopies, some net energy may be transferred between light and matter, even as one focuses experimentally not on population changes in the material, but on alterations of the radiation. Class II events include all of the resonant and nonresonant, linear and nonlinear *dispersions*. Examples of Class II spectroscopies are classical diffraction and reflection (strongest at the linear level) and a whole array of light-scattering phenomena like frequency summing (harmonic generation), frequency differencing, free induction decay, and optical echoes.

To be general, we anticipate that the incident field may be composed of many components as defined in the laboratory by their amplitude, their colors or frequencies (dc components are considered a special case), their polarizations, their time history, and their wave vectors. The incident field is of course pure real and so are its components. But it proves convenient to express each component field mathematically as a sum of its complex (analytical) form and the conjugate (see below). Before introducing techniques for classifying any given spectroscopy, a summary of some general distinguishing properties of these two Classes is offered in Table 1.

From the start it is helpful to recognize that when the field interacts with the material, to one extent or another, all of these spectroscopies take place simultaneously. It is the scientist, who by experimental design of the incident field and selected signal properties, that defines one (or at most a few) of the many classifiable spectroscopies.

The most complete theoretical treatment of the light−matter problem is achieved by applying statistical quantum mechanics

† Present address: Department of Chemistry, Concordia College, Moorhead, MN 56562.

10.1021/jp992542c CCC: $19.00
Published on Web 11/18/1999

TABLE 1: Distinguishing Properties of the Two Classes of Spectroscopies

Class I	Class II
Always require resonances. Nonresonant interferences are absent.	May or may not contain resonances. Nonresonant terms are always present. Interference between resonant and nonresonant polarizations is present. Cross terms between them appear when *homodyne* detected.
Invariably "self-heterodyned". The polarization field necessarily finds its conjugate among the components of the incident field (see text). The remaining components also act as conjugate pairs. The light−matter interaction is then said to be maximally "in quadrature". This means that Class I spectroscopies can appear only at *odd* order in the incident field. For this reason, the electric polarization must carry the same frequency, wavelength, and wave vector as the odd, unpaired component. Thus, the simple "photon" picture of the spectroscopy becomes natural.	Can appear at *all* orders of the incident field [but only at *odd* orders for achiral isotropic media (gases, liquid, amorphous solids)]. At *even* order, the polarization (the signal) field must oscillate at a new frequency not present in the incident field. At odd order, the polarization field may contain frequency components of the incident field but usually produces a new color.
Cross-section is *linear* in concentration of the resonant species.	Cross-section is *quadratic* in concentration for homodyne detection; *linear* for heterodyne detection.
Phase-matching is automatic because self-heterodyned. It need not be implemented by design.	Phase-matching must be implemented through experimental design.

in the form of the time evolution of the light−matter *density operator* [see, for example, refs 3−6]. A diagrammatic approach can unify the theory underlying all of the spectroscopies, thus aiding in their classification and their sorting. Two common and completely synonymous diagrammatic techniques are the dual Feynman diagrams[5,6] and the wave-mixing energy level (WMEL) diagrams. The latter shall be used here.[1,2]

As we shall see, it also proves useful to regard *time-ordered* products of naturally occurring complex field factors as "generators" of spectroscopies at any given order. Each of these generators is associated with its own complete set of density operator evolution diagrams (Feynman or WMEL) to provide a complete view of any given spectroscopy. To illustrate, we use these tools to isolate and classify 30 Raman spectroscopies that can be found (under a variety of acronyms) in the current literature.

II. A General Approach toward Classifying the Spectroscopies

A. Perturbative Development of the Electrical Polarization. Once the density operator is known at any time and position within a material, its matrix in the eigenstate basis set of the constituents (usually molecules) can be determined. The ensemble averaged electrical polarization, **P**, is then obtained. It is the centerpiece of all spectroscopies based on the electric component of the EM field.

This oscillating electric dipole density, **P** (the polarization), produced by the total incident electric field, **E**, generates all of the spectroscopies, both linear and nonlinear as well as Classes I and II. The energy contained in **P** may be used in part (or altogether) to shift the population of energy states of the material, or it may in part (or altogether) reappear in the form of a new EM field oscillating at the frequency of the induced polarization. When the population changes, or energy loss or gain in the light is detected, one is engaged in a Class I spectroscopy. On the other hand, when properties of the new field are being measured—such as its frequency, direction (wave vector), state of polarization, and amplitude (or intensity)—one is undertaking a Class II spectroscopy.

The induced polarization treated perturbatively is given by

$$\mathbf{P} = \overbrace{X^{(1)}\mathbf{E}}^{\mathbf{P}^{(1)}} + \overbrace{X^{(2)}\mathbf{EE}}^{\mathbf{P}^{(2)}} + \overbrace{X^{(3)}\mathbf{EEE}}^{\mathbf{P}^{(3)}} + \ldots \overbrace{X^{(s)}\mathbf{E}\ldots\mathbf{E}}^{\mathbf{P}^{(s)}} + \ldots \quad (1)$$

where the successive terms clearly appear with increasing order of nonlinearity in the total field, **E**. At this point, all properties appearing in eq 1 are mathematically pure real. The response function of the material to the electric field acting at *s*th order is the electrical susceptibility, $X^{(s)}$ (it is an $(s+1)$ rank tensor). Each element of this tensor will carry $(s+1)$ subscripts, a notation that is used, understandably, only when necessary. Furthermore, the events at the *s*th order, are sometimes referred to as "$(s+1)$-wave-mixing"—the additional field being the new EM field derived from $\mathbf{P}^{(s)}$.

All *nonlinear* (electric field) spectroscopies are to be found in all terms of eq 1 except for the first. The latter exclusively accounts for the standard linear spectroscopies—one photon absorption and emission (Class I) and linear dispersion (Class II). The term at third order contains by far the majority of the modern nonlinear spectroscopies.

As noted, it is the laboratory configuration of an experiment that focuses on one particular kind of spectroscopy, even while all possible light−matter events must be occurring in the sample. How can one isolate a spectroscopy of interest from eq 1? We shall see how passage to the complex mathematical representation of the various properties is invaluable in this process. It is useful to start by addressing the issue of distinguishing Class I and Class II spectroscopies at any given order of nonlinearity.

B. Class I and Class II Spectroscopies and the Appearance of the Complex Susceptibilities. All Class I spectroscopies at any order can be exposed by considering the long-term exchange of energy between light and matter as judged by the nonvanishing of the induced power density over many cycles of the field. The instantaneous power density at *s*th order is given by $\{\mathbf{E}\cdot(\partial\mathbf{P}^{(s)}/\partial t)\}$. For this product to survive over time, the normalized integral over a time *T*, which is much longer than the optical period of the field, should not vanish. This is called the cycle averaged, *s*th order power density. It is expressed as

$$W^{(s)} = \frac{1}{T}\int_0^T \mathrm{d}t \left\{\mathbf{E}\cdot\frac{\partial\mathbf{P}^{(s)}}{\partial t}\right\} \quad (2)$$

For $W^{(s)} > 0$, one has absorption; for $W^{(s)} < 0$, emission. Multiphoton absorption and emission fall into this Class. Though $\mathbf{P}^{(s)}$ involves *s* actions of the total field, the light−matter energy exchange is always in the language of photons. A net energy in the form of photons is destroyed (absorbed) as the quantum state population of the material moves upward in energy; a net energy in the form of photons is created (emitted) as the population moves downward in energy. To survive the integration over the long time integral *T*, the instantaneous power density cannot oscillate rapidly (if at all), certainly not at optical frequencies. Since **E** is intended to consist entirely of fields that oscillate at optical frequencies, the power density can have a nonoscillating term only when the field appears altogether an *even* number of times. Since it appears *s* times in $\mathbf{P}^{(s)}$ (eq 1) and once in **E**, all Class I spectroscopies exist only when $(s+1)$ is even or when *s* is odd (see eq 2 and Table 1).

Furthermore, the nonoscillating component of the integrand can best be sorted out by going to the complex representation of the total field, the polarization, and the susceptibility. The

mathematically pure real quantities in eq 1 are written in their complex representation as

$$\mathbf{E} = {}^1/_2(\boldsymbol{\varepsilon} + \boldsymbol{\varepsilon}^*) \tag{3}$$

$$\mathbf{P}^{(s)} = {}^1/_2(\mathbf{p}^{(s)} + (\mathbf{p}^{(s)})^*) \tag{4}$$

$$X^{(s)} = {}^1/_2(\chi^{(s)} + (\chi^{(s)})^*) \tag{5}$$

in which $\boldsymbol{\varepsilon}$, $\mathbf{p}^{(s)}$, and $\chi^{(s)}$ are, in general, complex quantities whose real parts are given by $\mathbf{E}$, $\mathbf{P}^{(s)}$, and $X^{(s)}$, respectively. By introducing eqs 3−5 into eq 2, and applying the cycle average theorem for the integral,[7] one finds that for all spectroscopies at *s*th order involving long-term light−matter energy exchange (Class I, in particular), the signal measured as a net energy exchange, $S_{\mathrm{I}}^{(s)}$, is proportional to the cycle averaged power density, or $S_{\mathrm{I}}^{(s)} \propto W^{(s)} \propto \mathrm{Im}\ \chi^{(s)}$. If the complex susceptibility, $\chi^{(s)}$, is actually pure real, there can be no long-term energy exchange between light and matter. Thus there can be no Class I spectroscopies based on a susceptibility component for which $\mathrm{Im}\ \chi^{(s)} = 0$.

Consider an ensemble composed of N constituents (such as molecules) per unit volume. The (complex) density operator for this system is developed perturbatively in orders of the applied field, and at *s*th order is given by $\rho^{(s)}$. The (complex) *s*th order contribution to the ensemble averaged polarization is given by the trace over the eigenstate basis of the constituents of the product of the dipole density operator, $N\mu$ and $\rho^{(s)}$: $\mathbf{p}^{(s)} = \mathrm{Tr}\{N\mu\rho^{(s)}\}$. In turn, an expression for $\chi^{(s)}$ is obtained, which in the frequency domain, consists of a numerator containing a product of $(s + 1)$ transition moment matrix elements and a denominator of s energy factors, which, when complex, express light−matter resonances and allow $\chi^{(s)}$ to become a complex quantity. Its Im $\chi^{(s)}$ part (pure real) is responsible for Class I spectroscopies. The light−matter resonances introduce the imaginary component to $\chi^{(s)}$ and permit a Class I spectroscopy to exist.

As noted, the Class II spectroscopies are based on detecting the new EM field that is derived from the induced polarization, $\mathbf{P}^{(s)}$ at *s*th order. Here $\mathbf{P}^{(s)}$ oscillating at optical frequencies, acts as the source term in Maxwell's equation to create the new optical field, $\mathbf{E}_{\mathrm{new}}$, at the same frequency. Again, we recognize $\boldsymbol{\varepsilon}_{\mathrm{new}} \propto \mathbf{p}^{(s)} \propto \chi^{(s)}$.

Since optical fields oscillate too quickly for direct detection, they must be measured "in quadrature"—as photons. There are two ways to achieve quadrature. One is *homodyne* detection in which the new field is measured at its quadrature, $\boldsymbol{\varepsilon}_{\mathrm{new}}\boldsymbol{\varepsilon}_{\mathrm{new}}^* = |\boldsymbol{\varepsilon}_{\mathrm{new}}|^2$. These signals must be proportional to $|\chi^{(s)}|^2$. Thus, $S_{\mathrm{II}}^{(s)}$ (*homodyne*) $\propto |\chi^{(s)}|^2$ and all phase information in $\chi^{(s)}$ is lost. Such is the case for almost all of the Class II spectroscopies.

The second way to achieve quadrature is to introduce another field, $\mathbf{E}_{\mathrm{lo}}$, (called a local oscillator) designed in frequency and wave vector to conjugate (go into quadrature) in its complex representation with the new field of interest. Thus, in the heterodyne case, the signal photons are derived from $\boldsymbol{\varepsilon}_{\mathrm{new}}\boldsymbol{\varepsilon}_{\mathrm{lo}}^*$ or $S_{\mathrm{II}}^{(s)}$ (*heterodyne*) $\propto \chi^{(s)}$. In heterodyne detected $(s + 1)$ wave-mixing, phase information is retained and one can take a full measure of the complex susceptibility, including its phase. The phase of the complex induced polarization, $\mathbf{p}^{(s)}$, determines how its energy will partition between Class I (absorbed or emitted) and Class II (a new EM wave is launched) spectroscopies.[2]

To anticipate the introduction of "generators", we consider all of the spectroscopies at third order ($s = 3$). To be otherwise as general as possible, suppose the total incident field consists of the combination of three experimentally distinct fields ($j = 1, 2, 3$). These can differ in any combination of their frequency, polarization, direction of incidence (wavevector), and time history. Thus, the total field is written as

$$\mathbf{E} = \sum_{j=1}^{3}\mathbf{E}_j \tag{6}$$

In using the complex representation (eq 3), the *j*th electric field is given as

$$\mathbf{E}_j = {}^1/_2(\boldsymbol{\varepsilon}_j + \boldsymbol{\varepsilon}_j^*) \tag{7}$$

where (using Euler's identity)

$$\boldsymbol{\varepsilon}_j = \mathbf{E}_j^0 \mathrm{e}^{-i(\mathbf{k}_j\cdot\mathbf{r}-\omega_j t)} \tag{8}$$

$$\boldsymbol{\varepsilon}_j^* = (\mathbf{E}_j^0)^* \mathrm{e}^{i(\mathbf{k}_j^*\cdot\mathbf{r}-\omega_j^* t)} \tag{9}$$

Here $|\mathbf{E}_j^0|$ is the amplitude of the *j*th field and the real part of ω_j is its (circular) frequency or "color". The real part of $\mathbf{k}_j$ is the product of the unit vector of incidence inside the sample, $\mathbf{e}_k$, and its amplitude, $2\pi n_j/\lambda_j$. Here λ_j/n_j is the wavelength of the *j*th field inside the sample—λ_j being the wavelength inside a vacuum and n_j being the (real) index of refraction of the sample at ω_j. As implied, all three properties may be complex. The amplitude because of an added phase to the field and/or a field that is elliptically (or circularly) polarized; the frequency because the field may be growing or decaying in time and the wavevector because the field may be decaying and growing according to its location within the sample.

The total field (eq 6 with eq 7) is now

$$\mathbf{E} = {}^1/_2\sum_{j=1}^{3}(\boldsymbol{\varepsilon}_j + \boldsymbol{\varepsilon}_j^*) \tag{10}$$

It is only a matter of inserting this "hexanomial", eq 10, into eq 1 to organize all possible three-beam spectroscopies that might appear at any given order.

C. The "Generators" from the Complex Representation of the Field: An Example at Third Order. By far most of the nonlinear spectroscopies appear at third order. The majority of the Raman spectroscopies, including spontaneous Raman scattering, are found there as well. In order to develop the theoretical structure that underlies these many spectroscopies, we use the above complex representation of the incident fields, to produce the "generators" of all possible electric field spectroscopies at third order. After this exercise, it will be a simple matter to isolate the subset that constitutes the entire family of Raman spectroscopies.

At third order, one must expand ${}^1/_8(\sum_{i=1}^3(\boldsymbol{\varepsilon}_i + \boldsymbol{\varepsilon}_i^*)\sum_{j=1}^3(\boldsymbol{\varepsilon}_j + \boldsymbol{\varepsilon}_j^*)\sum_{k=1}^3(\boldsymbol{\varepsilon}_k + \boldsymbol{\varepsilon}_k^*))$ to enumerate the "generators" of all possible third order spectroscopies. In this case, any given generator consists of an ordered product of these complex fields, such as $\boldsymbol{\varepsilon}_i\boldsymbol{\varepsilon}_j\boldsymbol{\varepsilon}_k^*$. The ordering of the fields in each generator represents a time ordering of the actions of the applied fields. This can be of physical significance. Clearly this expansion must give 216 terms (6^3). These 216 terms or generators can be arranged into 108 pairs of mutually conjugate generators, since the total electric field is itself a quantity that is pure real. Of these 108 paired terms, exactly 27 are in the category of what is termed *nondegenerate* four-wave-mixing (ND4WM), where the signal frequency must be very far from any of the incident optical frequencies. These 27 pairs can generate only Class II spec-

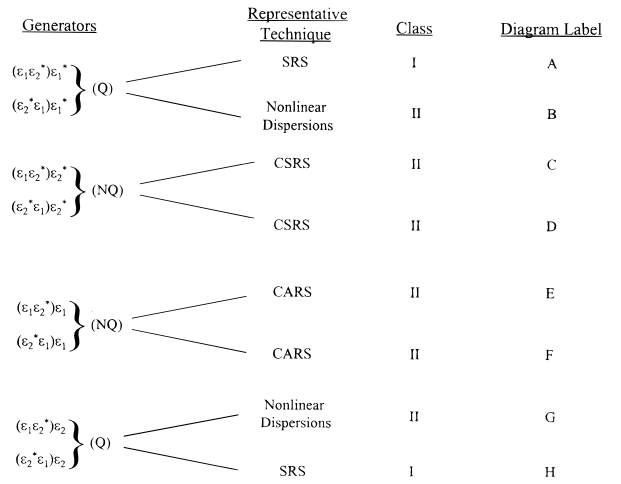

Figure 1. Eight third order, two-color, Raman generators. Their full quadrature (Q) or nonquadrature (NQ) is indicated. The acronym of one of the related Raman spectroscopies is given, and each is labeled by spectroscopic Class. Finally each generator is identified according to its Window stage WMEL diagram [found alphabetically labeled in the second column of Figure 2a,b].

troscopies and (it turns out) none of the Raman spectroscopies. The generic pair for these ND4WM processes is $\boldsymbol{\varepsilon}_i\boldsymbol{\varepsilon}_j\boldsymbol{\varepsilon}_k$, + $\boldsymbol{\varepsilon}_i^*\boldsymbol{\varepsilon}_j^*\boldsymbol{\varepsilon}_k^*$, where each of *i*, *j*, or *k* can be fields 1, 2, or 3. (Henceforth the factor of $^1/_8$ shall be suppressed since it is common to all 216 generators.) The simple algebra of exponents is applied to such a product using eqs 8 and 9. Thus, one sees how the polarization wave generated from such a term must oscillate at a frequency much larger than any of the incident colors, namely, at the (real part of) $\omega_p = \omega_i + \omega_j + \omega_k$. The polarization wave must have a wave vector given by

$$\begin{aligned} \mathrm{Re}(\mathbf{k}_p) &= \mathrm{Re}(\mathbf{k}_i + \mathbf{k}_j + \mathbf{k}_k) \qquad (11) \\ &= 2\pi((n_i/\lambda_i)\mathbf{e}_{\mathbf{k}_i} + (n_j/\lambda_j)\mathbf{e}_{\mathbf{k}_j} + (n_k/\lambda_k)\mathbf{e}_{\mathbf{k}_k}) \end{aligned}$$

The appropriate (complex) susceptibility tensor for this generator is $\chi^{(3)}(\omega_p{=}\omega_i{+}\omega_j{+}\omega_k)$.

When resonances, or near resonances, are present in the 4WM process, the ordering of the field actions in the perturbative treatment (eq 1), can be highly significant. Though the three-color generators ($\boldsymbol{\varepsilon}_i\boldsymbol{\varepsilon}_j\boldsymbol{\varepsilon}_k$, $\boldsymbol{\varepsilon}_j\boldsymbol{\varepsilon}_k\boldsymbol{\varepsilon}_i$, $\boldsymbol{\varepsilon}_k\boldsymbol{\varepsilon}_i\boldsymbol{\varepsilon}_j$, ...) have identical frequency and wavevector algebra, their associated susceptibility functions [$\chi^{(3)}(\omega_p{=}\omega_i{+}\omega_j{+}\omega_k)$, $\chi^{(3)}(\omega_p{=}\omega_j{+}\omega_k{+}\omega_i)$, $\chi^{(3)}(\omega_p{=}\omega_k{+}\omega_i{+}\omega_j)$, ...], are, in general, different. As a result of the different color ordering, two of their three energy denominator factors must differ. For this reason, the field ordering in each generator, together with its own response function, must be regarded individually.

The fourth electromagnetic wave, $\mathbf{E}_{\mathrm{new}}$, shall henceforth be called the signal wave, $\mathbf{E}_s = {}^1/_2(\boldsymbol{\varepsilon}_s + \boldsymbol{\varepsilon}_s^*)$. It always must carry the same frequency as that of the polarization wave ($\omega_p = \omega_s$). It is launched by the collapse of this wave, provided that the polarization extends coherently over at least a few wavelengths of the incident light and that $\mathbf{k}_p = \mathbf{k}_s$.

The latter condition corresponds to the phase matching requirement already mentioned—the wavelength and direction of the material polarization wave must match that of the new EM wave as closely as possible. However for all Class I spectroscopies, this condition is automatically achieved because these are self-heterodyned or are automatically in quadrature.

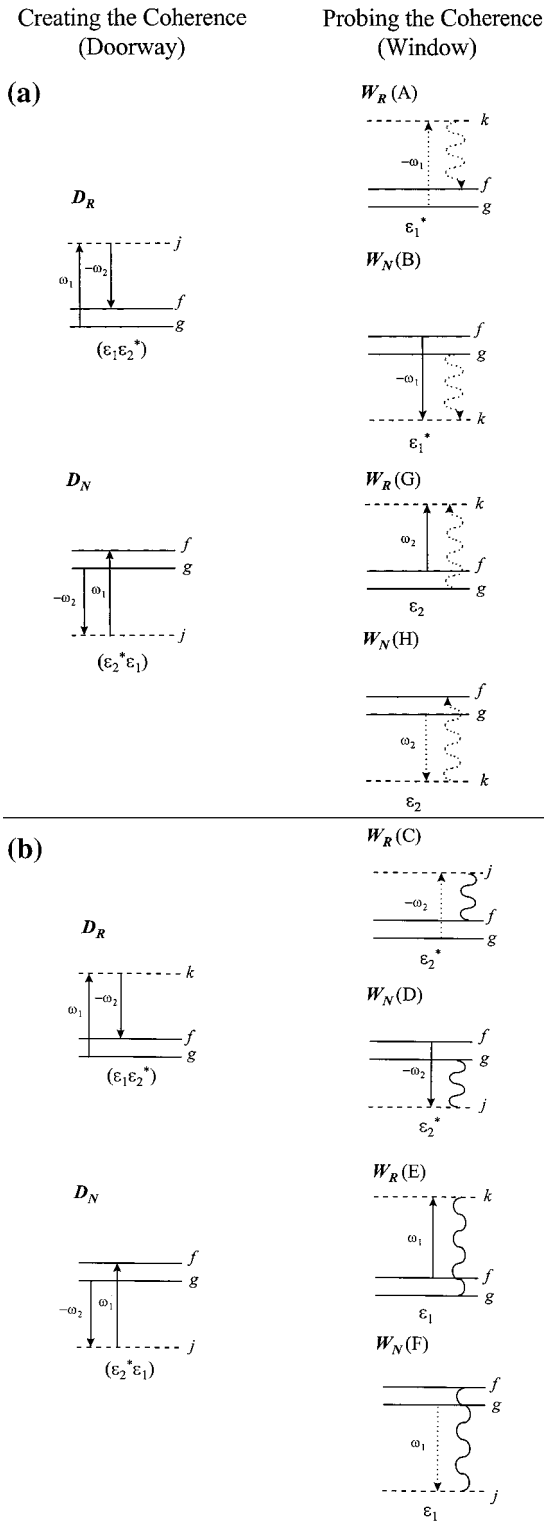

Figure 2. Separate WMEL diagrams for the Doorway and Window stages of the Raman spectroscopies. Solid and dashed vertical arrows correspond to ket- and bra-side light−matter interactions, respectively. The signal field is denoted by the vertical wavy line (arrow). The ground and final molecular levels (solid horizontal lines) are labeled *g* and *f*, while the virtual levels (dashed horizontal lines) are labeled *j* and *k*. The associated generators are given below each diagram. The Doorway/Window stages are classified as potentially resonant (D_R/W_R) or certainly nonresonant (D_N/W_N). In addition, the Window stages are labeled alphabetically in order to distinguish the Raman techniques by their Window stage WMEL diagram(s) (as in Tables 2 and 3 and Figure 1). (a) The Doorway and Window stage WMEL diagrams for SR, SRS, and RRS; (b) Doorway and Window stage WMEL diagrams for CARS and CSRS.

In fact, this is true for all "quadrature" spectroscopies—the Class I spectroscopies being the principal such. But, as noted, phase matching is a nontrivial requirement in the "nonquadrature" Class II spectroscopies, particularly in optically dispersive media.

In the complex mathematical representation, "quadrature" means that, at the $(s + 1)$ wave-mixing level, the product of s input fields constituting the sth order generator and the signal field can be organized as a product of $(s + 1)/2$ conjugately paired fields. Such a pair for field i is given by $\boldsymbol{\varepsilon}_i\boldsymbol{\varepsilon}_i^* = |\boldsymbol{\varepsilon}_i|^2$. One sees that the exponent algebra for such a pair removes all dependence on the $\mathrm{Re}(\omega_i)$ and $\mathrm{Re}(\mathbf{k}_i)$, thus automatically removing all oscillations as well as satisfying the phase-matching requirement. A necessary (but not sufficient) requirement for full quadrature is for s to be odd and also that half of the $(s + 1)$ fields be found to act conjugately with respect to the other half. Thus, for $(s + 1)$ fields, whenever the number of nonconjugate fields differs from the number of conjugate fields, one can only have "nonquadrature". Phase matching then must become an issue. This must always be the case for odd-wave-mixing (s is even), and it is also true for the above set of 27 frequency summing generators (for ND4WM). Thus for the presently considered generator, $\boldsymbol{\varepsilon}_i\boldsymbol{\varepsilon}_j\boldsymbol{\varepsilon}_k$, all three fields ($i$, j, and k) act nonconjugately, so quadrature at the four-wave level simply is not possible.

D. The Spectroscopies at Third Order According to Field Generators. The Raman Spectroscopies Isolated. We are now prepared to uncover all of the third order Raman spectroscopies and, in doing so, indicate how one might proceed to reveal the Raman events at higher order as well. Of the 108 pairs of conjugate generators, the remaining 81, unlike the above 27, are characterized by having one of the three fields acting conjugately with respect to the remaining two. Nine of these 81 terms generate fully degenerate 4WM. They constitute the "one-color" terms: $\boldsymbol{\varepsilon}_i^*\boldsymbol{\varepsilon}_i\boldsymbol{\varepsilon}_i$ + cc, $\boldsymbol{\varepsilon}_i\boldsymbol{\varepsilon}_i^*\boldsymbol{\varepsilon}_i$ + cc, and $\boldsymbol{\varepsilon}_i\boldsymbol{\varepsilon}_i\boldsymbol{\varepsilon}_i^*$ + cc ($i =$ 1, 2, or 3) with susceptibility $\chi^{(3)}(\omega_s = \omega_i)$, since $\omega_s = -\omega_i + \omega_i + \omega_i = \omega_i$ with wavevector $\mathbf{k}_s = -\mathbf{k}_i + \mathbf{k}_i = \mathbf{k}_i$. Their full degeneracy is evident since all four fields carry the same frequency (apart from sign). Resonances appear in the electric susceptibilities when, by choice of incident colors and their signs, one or more of their energy denominators (s in number at sth order) approaches a very small value because the appropriate algebraic color combination matches Bohr energies (material energy gaps) of the material. When considering the subgroup of all Raman spectroscopies, by definition, the susceptibility must contain at least one resonance that involves a small Bohr frequency. When using only optical frequencies, this can only be achieved by having two fields act conjugately and possess a difference frequency that matches the low-frequency material resonance. Further, they must act in the first two steps along the path to the third order polarization of the sample. These first two steps together prepare the Raman resonant material coherence and can be referred to as the "Doorway" stage of the Raman 4WM event.

Suppose the incident colors are such that the required Raman resonance (ω_R) appears at $\omega_1 - \omega_2 \approx \omega_R$ (with $\omega_1 > \omega_2$). Thus, the appropriate generators for the two-step Doorway stage, common to all of the Raman spectroscopies, must be $\boldsymbol{\varepsilon}_1\boldsymbol{\varepsilon}_2^*$ and $\boldsymbol{\varepsilon}_2^*\boldsymbol{\varepsilon}_1$, (and their conjugates, $\boldsymbol{\varepsilon}_1^*\boldsymbol{\varepsilon}_2$ and $\boldsymbol{\varepsilon}_2\boldsymbol{\varepsilon}_1^*$). These differ only in the permutation of the ordering of the actions of fields 1 and 2. The usual algebra of exponents tells us that this Doorway stage produces an intermediate polarization that oscillates at $\omega_1 - \omega_2 \approx \omega_R$. The resonantly produced Raman coherence having been established, it remains only to probe this intermediate polarization, that is, to convert it into an optical polarization from which the signal at optical frequencies is prepared. This is accomplished by the action of the third field which converts the low-frequency Raman coherence into an optical one. This, in turn, leads to the signal. This last two-step event can be referred to as the "Window" stage of the 4WM process. Obviously there are at most only six possible choices for this third field: $\boldsymbol{\varepsilon}_j$ and $\boldsymbol{\varepsilon}_j^*$ with $j = 1, 2, 3$. In this way we have isolated from the original 108 4WM generators the 12 that are responsible for all of the Raman spectroscopies. The choice of the probe field determines the frequency of the signal as well as its wave vector. While all types of Raman signals must be present at some level of intensity in any given experiment, it is again a matter of experimental design—the detected ω_s and the aperture-selected $\mathbf{k}_s$—as to which one Raman spectroscopy is actually being studied.

This classification by field generators in the complex field representation goes a long way toward organizing the nonlinear spectroscopies that carry at least one resonance. However it must be remembered that in emphasizing a field ordering that locates the essential Raman resonance, we have neglected any other possible resonant and all nonresonant contributions to the third order polarization. While any additional resonance(s) are important to both Class I and Class II spectroscopies, the nonresonant contributions play no role in class I spectroscopies but must not be ignored in Class II studies. If one starts with the generator $\boldsymbol{\varepsilon}_1\boldsymbol{\varepsilon}_2^*\boldsymbol{\varepsilon}_3$ and then permutes the ordering of the three distinct complex field amplitudes, one arrives at 6 (3!) generators, only two of which induce the Raman resonance at $\omega_1 - \omega_2 \approx \omega_R$ ($\boldsymbol{\varepsilon}_1\boldsymbol{\varepsilon}_2^*\boldsymbol{\varepsilon}_3$ and $\boldsymbol{\varepsilon}_2^*\boldsymbol{\varepsilon}_1\boldsymbol{\varepsilon}_3$). The remaining four can only polarize the material without this Raman resonance ($\omega_3 \neq \omega_1, \omega_2$), but if otherwise resonant, they can interfere with the Raman lineshape. Also when the issue of time-resolved spectroscopies arises, the time ordering of field actions is under experimental control, and the active field generators are limited not only by requirements of resonance but by their actual time ordering in the laboratory.

In any case, the polarizing action upon the material by a given generator must be followed in more detail. In density matrix evolution, each specified field action transforms either the "ket" or the "bra" side of the density matrix. Thus, for any specified sth order generator, there can be 2^s detailed paths of evolution. In addition, evolution for each of the $s!$ generators corresponding to all possible field orderings must be considered. One then has altogether $2^s s!$ paths of evolution. For $s = 3$ there are 48—eight for each of six generators. These paths are fully captured by the WMEL diagrams.

E. An Application: The Classification of 30 Raman Spectroscopies. The general task is to trace the evolution of the third order polarization of the material created by each of the above 12 Raman field operators. For brevity, we choose to select only the subset of 8 that is based on two colors only—a situation that is common to almost all of the Raman spectroscopies. Three-color Raman studies are rather rare, but are most interesting, as demonstrated both at third and fifth order by the work in Wright's laboratory.[8−11] That work anticipates variations that include infrared resonances and the birth of doubly resonant vibrational spectroscopy (DOVE) and its two-dimensional Fourier transform representations analogous to 2-D NMR.[12−14]

Interestingly, three-color spectroscopies at third order can only be of Class II, since the generators cannot possibly contain any quadrature. The maximal quadrature necessary for Class I is impossible.

For the two-color spectroscopies, maximal quadrature is possible and both Class I and Class II events are accounted for.

TABLE 2: Class I[a] Raman Spectroscopies

Technique	Acronym	Representative WMEL Window diagram(s)[b]
Third Order		
spontaneous Raman	SR	A,B
stimulated Raman gain spectroscopy	SRS	A,B,G,H
stimulated Raman loss spectroscopy	SRL	not shown
surface-enhanced Raman scattering	SERS	A,B
Fourier transform surface-enhanced Raman scattering	FT-SERS	A,B
Fourier transform spontaneous Raman	FT-SR	A,B
Hardamard transform Raman scattering	HTRS	A,B
resonance Raman scattering	RRS	A,B (D_R only)
dissociative resonance Raman scattering	DRRS	A,B (D_R only)
transient resonance Raman spectroscopy	TRRS	A,B (D_R only)
time resolved resonance Raman scattering	TRRR	A,B (D_R only)
photoacoustic spontaneous Raman spectroscopy	PARS	A,B
optoacoustic Raman spectroscopy	OARS	A,B
Fifth Order		
hyper-Raman scattering	HRS	not shown
surface-enhanced hyper-Raman scattering	SEHRS	not shown
surface-enhanced resonance hyper-Raman scattering	SERHRS	not shown

[a] The Class of a particular spectroscopy determines the general quantities that can be measured by a given technique—although the choice of a given spectroscopy depends greatly on experimental considerations and the expertise and/or resources of the experimenter. That being said, Class I or full quadrature spectroscopies have the potential to measure Raman frequencies, differential cross-sections, depolarization ratios, and Raman line shapes. Class II spectroscopies, in addition to potentially measuring the same quantities as that in Class I, have the added features of greater control over the signal (highly directional) and measurement of the resonant−nonresonant ratio for the electric susceptibility. [b] The wave-mixing energy level (WMEL) diagrams represent a specific Liouville pathway for the evolution of the density operator. The lettered diagrams listed here refer to the "Window" stage (W) of a particular WMEL diagram, as discussed in the text, since the "Doorway" stages (D) are common to all spectroscopies (unless otherwise noted). The diagrams for these Doorway and Window stages are given in Figure 2.

TABLE 3: Class II[a] Raman Spectroscopies

Technique	Acronym	representative WMEL Window diagram(s)[b]
Second Order		
coherent scattering UV/IR from chrial molecules in random media		not shown
Third Order		
coherent Raman scattering	CRS	C,D,E,F
interferometric coherent Raman scattering	$I^{(2)}$CRS	C,D,E,F
coherent anti-Stokes Raman scattering	CARS	E,F
interferometric coherent anti-Stokes Raman scattering	$I^{(2)}$CARS	E,F
coherent Stokes Raman scattering	CSRS	C,D
interferometric coherent Stokes Raman scattering	$I^{(2)}$CSRS	C,D
coherent Raman ellipsometry	CRE	C,D,E,F
Raman induced Kerr effect spectroscopy	RIKES	B,G
impulsive stimulated Raman scattering	ISRS	C,D,E,F
Fourth Order		
BioCARS	BioCARS	not shown
Fifth Order		
Raman quasi-echo	RQE	not shown
coherent higher order Raman excitation spectroscopy	CHORES	not shown
coherent hyper-Raman scattering	CHRS	not shown
Seventh Order		
Raman echo	RE	not shown

[a] See footnote a in Table 2. [b] See footnote b in Table 2.

Thus, we trace diagrammatically the evolution to produce a signal field caused by the eight generators: (i) the four $(\boldsymbol{\varepsilon}_1\boldsymbol{\varepsilon}_2^*)\boldsymbol{\varepsilon}_1^*$, $(\boldsymbol{\varepsilon}_1\boldsymbol{\varepsilon}_2^*)\boldsymbol{\varepsilon}_2^*$, $(\boldsymbol{\varepsilon}_1\boldsymbol{\varepsilon}_2^*)\boldsymbol{\varepsilon}_1$, and $(\boldsymbol{\varepsilon}_1\boldsymbol{\varepsilon}_2^*)\boldsymbol{\varepsilon}_2$ and (ii) the four with the first two fields permuted, $(\boldsymbol{\varepsilon}_2^*\boldsymbol{\varepsilon}_1)\boldsymbol{\varepsilon}_1^*$, $(\boldsymbol{\varepsilon}_2^*\boldsymbol{\varepsilon}_1)\boldsymbol{\varepsilon}_2^*$, $(\boldsymbol{\varepsilon}_2^*\boldsymbol{\varepsilon}_1)\boldsymbol{\varepsilon}_1$, and $(\boldsymbol{\varepsilon}_2^*\boldsymbol{\varepsilon}_1)\boldsymbol{\varepsilon}_2$.

In each case we have indicated the Doorway stage using parentheses. We note how in each of the two groups (i and ii) of the four generators, the "outer" two are "maximally in quadrature" and may reach full quadrature depending on the conjugation of the signal fields. Also in each group of four, the inner two generators contain no quadrature among the three fields, so these can only lead to nonquadrature 4WM and therefore only to Class II spectroscopies, regardless of the conjugation of the signal field. As already noted, the generators that are fully conjugate to these eight need not be considered, for in the end we can always take the real part of the complex polarization produced by a given generator.

In Figure 1, these eight generators are organized for both the $(\boldsymbol{\varepsilon}_1\boldsymbol{\varepsilon}_2^*)$ and the $(\boldsymbol{\varepsilon}_2^*\boldsymbol{\varepsilon}_1)$ Doorway stages. Their potentially full-quadrature (Q) or their certain nonquadrature (NQ) is indicated. Further, their spectroscopic Class is identified—all of the NQ generators necessarily are assigned to Class II. The two potentially quadrature type generators may be assigned either to Class I or to Class II. The Raman spectroscopic examples of each are given. Finally, each is identified with its separate, alphabetically labeled, Window stage WMEL diagram. These diagrams are discussed next.

For $s = 3$, the time evolution of the system is tracked by following the stepwise changes in the bra-state, $\langle j|$, or the ket

state, $|k\rangle$, of the system caused by each of the three successive field interventions. This perturbative evolution of the density operator, or of the density matrix, is conveniently depicted diagrammatically using double sided Feynman diagrams or, equivalently, the WMEL diagrams. The latter are often preferred since light−matter resonances are explicitly exposed. In WMEL diagrams, the energy levels of the constituents of the matter are laid out as solid horizontal lines to indicate the states (called "real") that are active in a resonance and as dashed horizontal lines (or no lines) when they serve as nonresonant ("virtual") states. The perturbative evolution of the density matrix is depicted using vertically oriented arrows for each of the field actions that appears in a given generator. These arrows are placed from left to right in the diagram in the same order as the corresponding field action in the generator. The arrow length is scaled to the frequency of the acting field. Solid arrows indicate evolution from the old ket (tail of arrow) to the new ket (head of arrow); dashed arrows indicate evolution from the old bra (tail of arrow) to the new bra (head of arrow). For a field acting nonconjugately, like $\boldsymbol{\varepsilon}_i$, the frequency is positively signed, ω_i and the arrow for a ket change points up and that for a bra change points down. When the field acts conjugately, $\boldsymbol{\varepsilon}_i^*$, the frequency is negatively signed, $-\omega_i$, and a ket changing arrow points down, while a bra changing arrow points up. These rules allow one to depict diagrammatically any and all density matrix evolutions at any order. Given the option of a bra or a ket change at each field action, one sees how a given *s*th order generator leads to 2^s diagrams, or paths of evolution. Normally only some (if any) encounter resonances. A recipe has been published[1] which allows one to translate any WMEL diagram into the analytic expression for its corresponding electrical susceptibility for continuous wave (cw) fields. After *s* arrows have appeared (for an *s*th order evolution), the $(s + 1)$th field is indicated for any WMEL diagram of the nonquadrature class by a vertical wavy *line segment* whose vertical length scales to the signal frequency. For the WMEL diagrams of the full quadrature sort, the $(s + 1)$th field must be conjugate to one of the incident fields, so the wavy segment becomes a wavy arrow; either solid (ket-side action) or dashed (bra-side action).

Of the four possible WMEL diagrams for each the $(\boldsymbol{\varepsilon}_1\boldsymbol{\varepsilon}_2^*)$ and $(\boldsymbol{\varepsilon}_2^*\boldsymbol{\varepsilon}_1)$ Doorway generators, only one encounters the Raman resonance in each case. We start with two parallel horizontal solid lines, together representing the energy gap of a Raman resonance. For ket evolution using $(\boldsymbol{\varepsilon}_1\boldsymbol{\varepsilon}_2^*)$, we start on the left at the lowest solid line (the ground state, *g*) and draw a long solid arrow pointing up $(+\omega_1)$, followed just to the right by a shorter solid arrow pointing down $(-\omega_2)$ to reach the upper solid horizontal line, *f*. The head of the first arrow brings the ket to a virtual state, from which the second arrow carries the ket to the upper of the two levels of the Raman transition. Since the bra is until now unchanged, it remains in *g* ($\langle g|$); this Doorway event leaves the density matrix at second order off-diagonal in which $\rho_{fg}^{(2)}$ is not zero. Thus, a Raman coherence has been made. Analogously, the $(\boldsymbol{\varepsilon}_2^*\boldsymbol{\varepsilon}_1)$ Doorway action on the ket side must be a short solid arrow down $(-\omega_2)$ from *g* to a virtual ket-state, and then long arrow up $(+\omega_1)$ to *f* from the virtual state. This evolution also produces $\rho_{fg}^{(2)}$. Both Doorway actions contain the same Raman resonance denominator, but differ in the denominator appearing at the first step: the downward $(\boldsymbol{\varepsilon}_2^*\boldsymbol{\varepsilon}_1)$ action is inherently antiresonant ("*N*" for nonresonant) in the first step; the upward $(\boldsymbol{\varepsilon}_1\boldsymbol{\varepsilon}_2^*)$ action is potentially resonant ("*R*" for resonant) in the first step and is therefore stronger. Accordingly, we distinguish these two Doorway events by labels D_N and D_R, respectively (see Figure 2). In resonance Raman spectroscopy, this first step in D_R is fully resonant and overwhelms D_N. (The neglect of D_N is known as the rotating wave approximation.) It is unnecessary to explore the bra-side version of these Doorway actions, for they would appear in the fully conjugate version of these Doorway events. Each of the Doorway steps, D_R and D_N, may be followed by any one of eight Window events. The WMEL diagrams for the Window events consist of the arrow for the last step of the third order polarization and the wavy segment for the signal wave. There are eight such Window diagrams since each of the two steps can involve two colors and either bra- or ket-side evolution. These eight Window WMEL diagrams are shown in Figure 2a,b and are identified alphabetically. These also carry potentially resonant and antiresonant properties in the third energy denominator (the first Window step) and accordingly are labeled W_R and W_N, where, as before, $W_R > W_N$. If the third step is completely resonant, $W_R \gg W_N$, and W_N may be completely neglected (as with $D_R \gg D_N$).

It is now possible to label all of the third order Raman spectroscopies (Tables 2 and 3 [many of these Raman spectroscopies are discussed in more detail with abundant literature citations in ref 15 to appear in 2000]) according to their essential Doorway/Window WMEL diagrams. This classification is shown in the third column of those tables. Again, the analytic form of the associated susceptibilities is obtained by recipe from the diagrams. When additional resonances are present, other WMEL diagrams must be included for both Class I and Class II spectroscopies. For the Class II spectroscopies, all of the nonresonant WMEL diagrams must be included as well.

Extension of this classification method to second, fourth, fifth, and higher orders follows directly (though the higher the order, the more complicated the enumerations). Tables 2 and 3 also include Raman events at even order, which are possible for chiral, but otherwise random, media.

Acknowledgment. We are most grateful for support from the National Science Foundation through Grant CHE-9616635.

References and Notes

(1) Lee, D.; Albrecht, A. C. In *Advances in Infrared and Raman Spectroscopy*; Clark, R. J. H., Hester, R. E., Eds.; Wiley: New York, 1985; Vol. 12, pp 179−213.

(2) Lee, D.; Albrecht, A. C. *Adv. Phys. Chem.* **1993**, *83*, 43−87.

(3) Cohen-Tannoudji, C.; Diu, B.; Laloë, F. *Quantum Mechanics*; Wiley: New York, 1977.

(4) Sakurai, J. J. *Modern Quantum Mechanics*; Addison-Wesley: Reading, MA, 1994.

(5) Mukamel, S. *Principles of Nonlinear Optical Spectroscopy*; Oxford University Press: New York, 1995.

(6) Shen, Y. R. *The Principles of Nonlinear Optics*; Wiley: New York, 1984.

(7) Loudon, R. *The Quantum Theory of Light*; Oxford University Press: New York, 1983.

(8) Wright, J. C.; Labuda, M. J.; Zilian, A.; Chen, P. C.; Hamilton, J. P. *J. Luminesc.* **1997**, *72*−*74*, 799−801.

(9) Labuda, M. J.; Wright, J. C. *Phys. Rev. Lett.* **1997**, *79*, 2446−2449.

(10) Wright, J. C.; Chen, P. C.; Hamilton, J. P.; Zilian, A.; Labuda, M. J. *Appl. Spectrosc.* **1997**, *51*, 949−958.

(11) Chen, P. C.; Hamilton, J. P.; Zilian, A.; Labuda, M. J.; Wright, J. C. *Appl. Spectrosc.* **1998**, *52*, 380−392.

(12) Tokmakoff, A.; Lang, M. J.; Larson, D. S.; Fleming, G. R. *Chem. Phys. Lett.* **1997**, *272*, 48−54.

(13) Tokmakoff, A.; Fleming, G. R. *J. Chem. Phys.* **1997**, *106*, 2569−2582.

(14) Tokmakoff, A.; Lang, M. J.; Larson, D. S.; Fleming, G. R.; Chernyak, V.; Mukamel, S. *Phys. Rev. Lett.* **1997**, *79*, 2702−2705.

(15) Kirkwood, J. C.; Ulness, D. J.; Albrecht, A. C. Raman Spectroscopy. In *The Encyclopedia of Chemical Physics and Physical Chemistry*; Moore, J. H., Spencer, N. D., Eds.; IOP Publishing: Philadelphia, in press.